Full Paper

Voltammetric Behavior of Antileukemia Drug Glivec. Part II – Redox Processes of Glivec Electrochemical Metabolite

Victor Constantin Diculescu,[a] *Marilene Vivan*,[b] *Ana Maria Oliveira Brett*[a]*

[a] Departamento de Química, Faculdade de Ciências e Tecnologia, Universidade de Coimbra, 3004-535 Coimbra, Portugal
[b] Hospital da Universidade de Coimbra, 3000 Coimbra, Portugal
*e-mail: brett@ci.uc.pt

Received: May 24, 2006
Accepted: June 28, 2006

Abstract
Glivec is a newly developed drug that belongs to the class of 2-phenylaminopyrimidine. It is a potent inhibitor of *ABL*-kinase, the main clinical manifestation of chronic myelogenous leukemia (CML). Based on its activity on CML, glivec is undergoing extensive evaluation for its activity against other tumor types. Detection and quantitation of glivec in biological fluids or cells is thus very important. The antileukemia drug glivec undergoes oxidation at glassy carbon electrodes and involves the formation of an oxidation product, P_{glivec}. The adsorption of P_{glivec} at the GCE surface yields a compact monolayer allowing an electrochemical study of this compound adsorbed at the GCE surface. The reversible redox reaction of the adsorbed P_{glivec} is pH dependent and occurs with the transfer of 2 electrons and 2 protons. The surface standard potential and the rate constant of the heterogeneous electrochemical reaction were calculated using cyclic voltammetry to be $E^{0'} = +180$ mV and $k = 15.5\ s^{-1}$, respectively. The total surface concentration of adsorbed P_{glivec} is 2.5×10^{-12} mol cm^{-2}. The analytical determination of glivec was carried out by differential pulse voltammetric measurement of the anodic peak current corresponding to either the oxidation peak of glivec or the oxidation peak of P_{glivec} adsorbed on the GCE surface. The limits of detection of glivec and adsorbed P_{glivec} based on three times the noise level are 3.3×10^{-8} M and 2.9×10^{-10} M, respectively.

Keywords: Glivec metabolite, Electrochemistry, Voltammetry, Standard potential, Rate constant, Adsorption

DOI: 10.1002/elan.200603592

1. Introduction

Glivec (Gleevec, STI 571, or imatinib mesylate) [1], Scheme 1, a derivative of 2-phenylaminopyrimidine, is a relatively small molecule with activity against protein tyrosine kinases [1, 2]. Glivec is an inhibitor of the *BCR-ABL* tyrosine kinase, a protein expressed by all patients with chronic myelogenous leukemia (CML) [4]. It is indicated for the treatment of patients with CML in blast crisis, accelerated phase, or in chronic phase after failure of interferon-α therapy [4]. Based on its activity on CML, glivec is undergoing extensive investigation for its activity against other tumor types [5, 6].

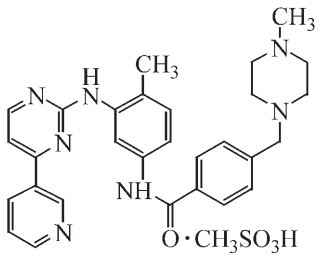

Scheme 1. Glivec chemical structure.

While the initial clinical results using glivec for the treatment of CML appear extremely promising, it was shown that problems such as the development of drug-resistant disease develop with prolonged usage [7–9]. In addition, the efficacy of glivec in producing molecular complete remissions may be improved using combinations with traditional antineoplastic agents [7]. As a result, there is an ongoing need for the determination of glivec pharmacokinetics so that issues such as drug–drug or drug-biomolecular complexes interactions can be evaluated. Detection and quantitation of glivec in organic fluids or cells is thus very important.

In order to support pharmacokinetic studies with sufficient speed, suitable analytical procedures are required. A semi-automated solid-phase extraction procedure with liquid chromatography–tandem mass spectrometry was an initial development [10]. A number of laboratories reported the use of high-throughput bioanalytical procedures using liquid chromatography–tandem mass spectrometry or UV detection [10–14] for analytical determination and quantitation of glivec in human plasma. There are also reports on a capillary zone electrophoretic method for the determination of glivec and its main metabolite in human urine [15].

Electroanalytical methods are inexpensive, fast, and an appropriate voltammetric method that can allow direct

measurements on biological samples with very little or no sample pretreatment. This is an enormous advantage when compared with other analytical techniques. Electroanalysis has been successfully used to quantitate different types of drugs, sometimes with very low detection limits [16].

Recently, it was shown that glivec and its main in vivo metabolite (*N*-demethylated piperazine derivative) are strongly adsorbed onto a static mercury electrode. By using this property and accumulating these compounds on a hanging mercury drop electrode (HMDE), square-wave voltammetry was used to achieve higher sensitivities [17]. However, there is a high tendency for the use of less toxic methodologies and a reduction in the use of organic solvents and mercury since they result in high ecological costs.

Therefore, the electrochemical study of adsorbed glivec and its oxidation product at a glassy carbon electrode (GCE) was carried out in an attempt to establish a new and sensitive procedure for the analytical determination of this compound. Glivec is oxidized at a GCE, and this process involves the formation of an electroactive product, P_{glivec}, which strongly adsorbs at the GCE, yielding a compact monolayer. The strong and irreversible adsorption of P_{glivec} at the electrode surface enables an electrochemical study of the adsorbed compound and a sensitive analytical determination of glivec can be achieved.

2. Experimental

2.1. Materials and Reagents

Glivec capsules of 100 mg obtained from Novartis (Portugal) were used without further purification. Stock solutions of 100 μM were prepared in purified water and stored at $-4\,^0$C. Solutions of different concentrations of glivec were prepared by dilution of the appropriate quantity in supporting electrolyte.

All supporting electrolyte solutions, Table 1, were prepared using analytical grade reagents and purified water from a Millipore Milli-Q system (conductivity ≤ 0.1 μS cm^{-1}).

Microvolumes were measured using EP-10 and EP-100 Plus Motorized Microliter Pipettes (Rainin Instrument Co. Inc., Woburn, USA). The pH measurements were carried out with a Crison micropH 2001 pH meter with an Ingold combined glass electrode. All experiments were done at room temperature ($25 \pm 1\,^0$C).

Table 1. Supporting electrolytes, 0.1 M ionic strength.

pH	Composition
2.6	HCl + KCl
3.6	HOAc + NaOAc
4.7	HOAc + NaOAc
5.5	HOAc + NaOAc
6.2	$NaH_2PO_4 + Na_2HPO_4$
7	$NaH_2PO_4 + Na_2HPO_4$
8.2	$NaH_2PO_4 + Na_2HPO_4$
9.5	$NaOH + Na_2B_2O_7$
12	NaOH + KCl

2.2. Voltammetric Parameters and Electrochemical Cells

Voltammetric experiments were carried out using a μAutolab running with GPES 4.9 software, Eco-Chemie, Utrecht, The Netherlands. The experimental conditions for differential pulse voltammetry (DPV) were: pulse amplitude 50 mV, pulse width 70 ms, scan rate 5 mV s^{-1}. Measurements were carried out using a glassy carbon electrode (GCE) ($d =$ 1.5 mm), with a Pt wire counter electrode, and a Ag/AgCl (3 M KCl) electrode as reference, in a 0.5 ml one-compartment electrochemical cell.

The GCE was polished using diamond spray (particle size 1 μm) before every electrochemical assay. After polishing, the electrode was rinsed thoroughly with Milli-Q water for 30 s; then it was sonicated for 1 minute in an ultrasound bath and again rinsed with water. After this mechanical treatment, the GCE was placed in buffer electrolyte and various DP voltammograms were recorded until a steady-state baseline voltammogram was obtained. This procedure ensured very reproducible experimental results.

2.3. Acquisition and Presentation of Voltammetric Data

All the voltammograms presented were background-subtracted and baseline-corrected using the moving average application with a step window of 5 mV included in GPES version 4.9 software. This mathematical treatment improves the visualization and identification of peaks over the baseline without introducing any artifact, although the peak intensity is in some cases reduced ($< 10\%$) relative to that of the untreated curve. Nevertheless, this mathematical treatment of the original voltammograms was used in the presentation of all experimental voltammograms for a better and clearer identification of the peaks. The values for peak current presented in all plots were determined from the original untreated voltammograms after subtraction of the base line.

2.4. Adsorption of Glivec Oxidation Product

The adsorption of the glivec oxidation product, P_{glivec}, at the GCE surface was carried out in a solution of 5 μM glivec in pH 7.2 0.1 M phosphate buffer following three procedures:

- Procedure 1: The clean GCE was placed in the solution of glivec, and several DP voltammograms were recorded between 0 and + 1.40 V until a stable P_{glivec} oxidation peak was recorded.
- Procedure 2: The clean GCE was held for 2 min in the solution of glivec at a potential of + 0.90 V;
- Procedure 3: After free adsorption for 2 min in the solution of glivec, the GCE was washed with a jet of

deionized water and then transferred to pH 7.2 0.1 M phosphate buffer where it was conditioned at +0.90 V during 2 min.

3. Results and Discussion

3.1. Adsorption of P_{glivec}

The antileukemia drug glivec adsorbs on the GCE surface. The first DP voltammogram obtained in pH 7.2 0.1 M phosphate buffer after adsorption of glivec showed, as described in Section 2.4, two oxidation peaks at $E^1_{pa} = +0.75$ V and $E^2_{pa} = +1.05$ V, respectively, Figure 1. On the second DP scan, a new anodic peak 3_a appeared at $E^3_{pa} = +0.22$ V. This peak corresponds to the glivec oxidation product, P_{glivec}, which strongly adsorbs on the electrode surface. Moreover, consecutively recorded DP voltammograms in buffer showed a very small decrease of peak 3_a corresponding to P_{glivec} oxidation current, only after 15 consecutive scans. Since no diffusion process occurs, disappearance of peaks 1_a and 2_a is due to total consumption of the glivec adsorbed onto the GCE after the first DP scan.

A detailed electrochemical study of the adsorbed P_{glivec} was carried out. For the optimization of adsorption conditions on the GCE surface, different procedures described in Section 2.4 were evaluated for various concentrations of glivec. After adsorption, the electrode was always washed with a jet of deionized water in order to remove the non-adsorbed molecules, and transferred to pH 7.2 0.1 M phosphate buffer where DP voltammograms were recorded. The voltammograms obtained with the three procedures were compared. Very reproducible results and higher oxidation peaks were obtained using Procedure 3, which was subsequently used to study the electrochemical behavior of P_{glivec} adsorbed on the GCE surface.

The adsorption of P_{glivec} from solutions with different concentrations of glivec was evaluated. The DP voltammograms were recorded in supporting electrolyte and the oxidation current of P_{glivec} was plotted vs. glivec concentration. Saturation of the electrode surface takes place at concentrations higher than 5 μM, Figure 2. For this reason, the adsorption of P_{glivec} was always carried out in a 5 μM glivec solution.

The determination of the degree of coverage of the electrode surface after adsorption of a specific compound is described by adsorption isotherms [19]. A number of isotherms have been proposed to describe adsorption equilibria at different electrode materials. From the results presented, it is difficult to determine the type of isotherm corresponding to the adsorbed P_{glivec} on the GCE surface. GCE is an isotropic material with amorphous characteristics. Thus, taking into account the existence of different types of surface adsorption sites and supposing there is no interaction between the adsorbed molecules, all conditions for a Temkin isotherm are fulfilled. As a particular case, if all adsorption sites are equal, a Langmuir isotherm would be obeyed [18]. However, it is correct, from the results obtained, to consider the formation of a monolayer of adsorbed P_{glivec} on the GCE surface.

3.2. Differential Pulse Voltammetry

The effect of pH on the oxidation peak potential, E_{pa}, and on the peak current I_{pa} of P_{glivec} adsorbed onto the GCE surface was studied using DPV in 0.1 M buffer supporting electrolytes with $1 < pH \leq 12$, Figure 3A.

The adsorption of P_{glivec} was carried out as described in Section 2.4, Procedure 3. The electrode was then placed in the electrolyte solution and the DP voltammogram was recorded immediately. Consecutive DPV scans in different

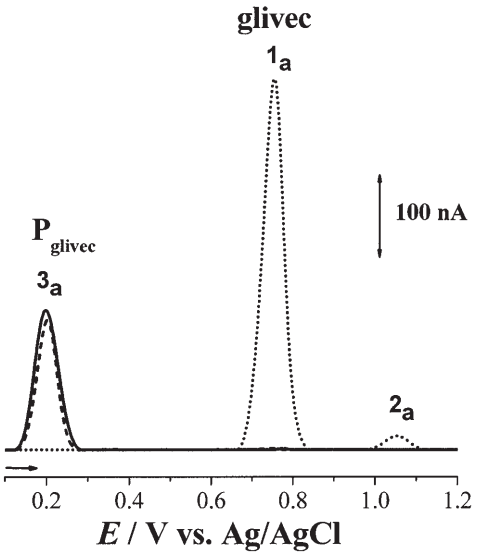

Fig. 1. DPV obtained with a GCE in pH 7.2 0.1 M phosphate buffer: (·····) 1st, (—) 2nd, and (– – – –) 15th scan after free adsorption during 2 minutes in a solution containing 5 μM glivec.

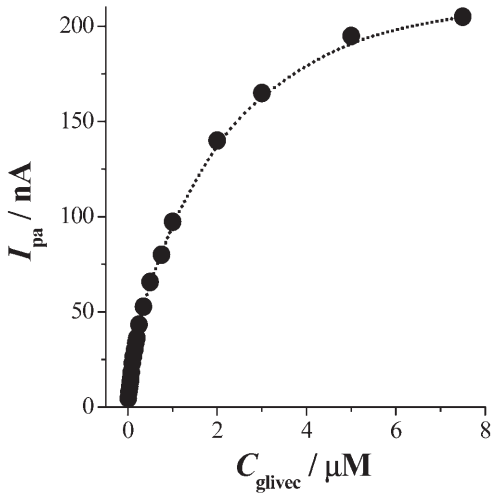

Fig. 2. Plot of I_{pa} of adsorbed P_{glivec} vs. glivec concentration in pH 7.2 0.1 M phosphate buffer. Adsorption of P_{glivec} at the GCE surface was carried out as described in Procedure 3, Section 2.4.

electrolyte solutions showed that the peak current is independent of the number of scans.

The oxidation of P_{glivec} is pH dependent and the variation of E_{pa} vs. pH is linear. The oxidation peak is displaced to lower potentials with increasing pH, Figure 3B. The slope of the line corresponds to 58 mV per pH unit, meaning that the same number of electrons and protons are involved in the oxidation mechanism. Nevertheless, in all electrolytes, the width at half height of the P_{glivec} oxidation peak was $W_{1/2} =$ 45 mV, which suggests that the oxidation of P_{glivec} occurs with the transfer of 2 electrons, hence also 2 protons.

Figure 3B also shows the variation of the oxidation peak current with the pH of the supporting electrolyte. The maximum current was observed in pH 7.2 0.1 M phosphate buffer. For this reason, this electrolyte was used for further investigations.

3.3. Cyclic Voltammetry

Cyclic voltammograms of P_{glivec} adsorbed onto the GCE surface were recorded in pH 7.2 0.1 M phosphate buffer for scan rates between 5 mV s^{-1} and 5 V s^{-1}. The adsorption was carried out as described in Section 2.4, Procedure 3. The voltammograms obtained for low scan rates, $5 \leq v \leq 250$ mV s^{-1}, presented symmetrical wave shapes that confirm the reversible character of P_{glivec} oxidation, Figure 4.

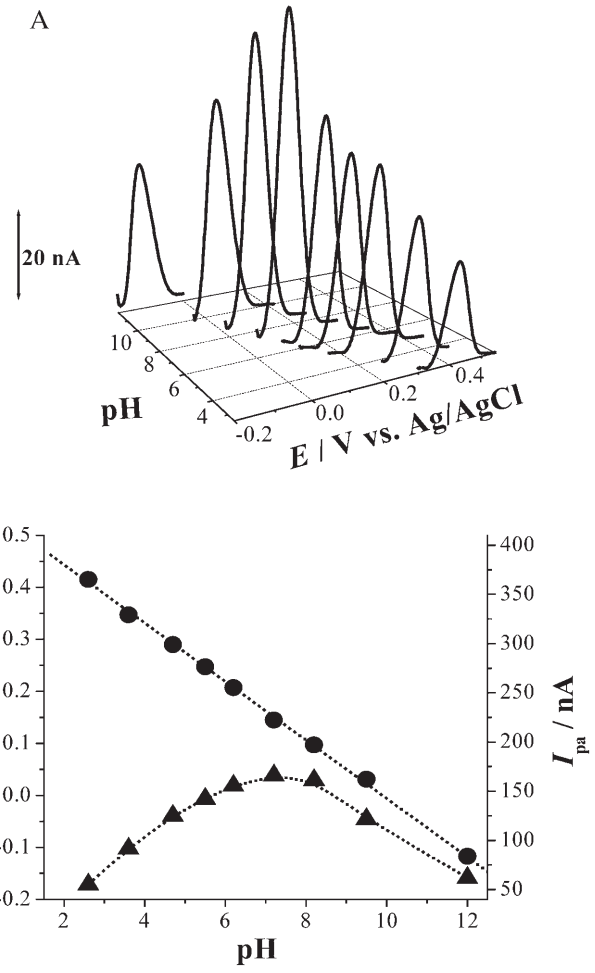

Fig. 3. A) 3D plot of DP voltammograms of adsorbed P_{glivec} as a function of pH. B) Plot of (●) E_{pa} and of (▲) I_{pa} of adsorbed P_{glivec} as function of pH.

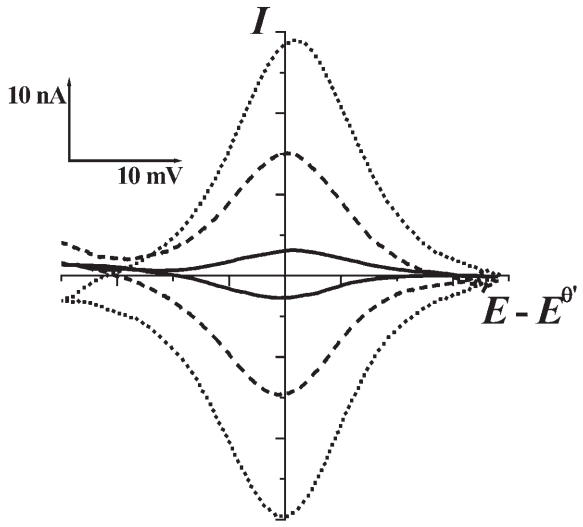

Fig. 4. Background-subtracted CV at (—) 5, (– – – –) 10, and (·····) 25 mV s^{-1} of adsorbed P_{glivec} in pH 7.2 0.1 M phosphate buffer.

For the lowest scan rate, $v = 5$ mV s^{-1}, $W_{1/2} = 48$ mV; hence, the number of electrons transferred is equal to 2 [19]. Considering the slope of the plot of peak potential versus pH, Figure 3B, the results obtained by DPV, that 2 electrons and 2 protons are exchanged during the redox reactions of P_{glivec}, are confirmed.

The wave shape symmetry, as well as the linear dependence of the anodic and cathodic currents with increasing scan rates observed, is a characteristic of electrode processes of organic species irreversibly adsorbed at the electrode surface and with reversible charge transfer kinetics in which the energy of the reagent and of the product are equal [18]. In these processes there is no contribution from the diffusion of the species in solution towards the electrode surface, since the voltammograms were recorded in supporting electrolyte. The slight asymmetry between the experimental voltammograms obtained and those predicted by the theory for adsorbed species stems from background supporting electrolyte interactions and from the non-ideal behavior of adsorbed species [20].

For higher scan rates, $v \geq 250$ mV s^{-1}, there is an increasing separation between the oxidation and the reduction peak potentials with increasing scan rate, showing the loss of system reversibility, the process becoming rate-limited, Figure 5. The small increase of the anodic and cathodic current peak width at half height, $W_{1/2}$, and of anodic and cathodic peak potential separation, ΔE_p, with increasing scan rate can be attributed to slower charge transfer kinetics for higher values of v [21].

Also, the peak currents increase with increasing scan rate. The nonlinear dependence of I_{pa} and I_{pc} for $v \geq 250$ mV s^{-1}, Figure 6A, is explained by considering the effect of very high

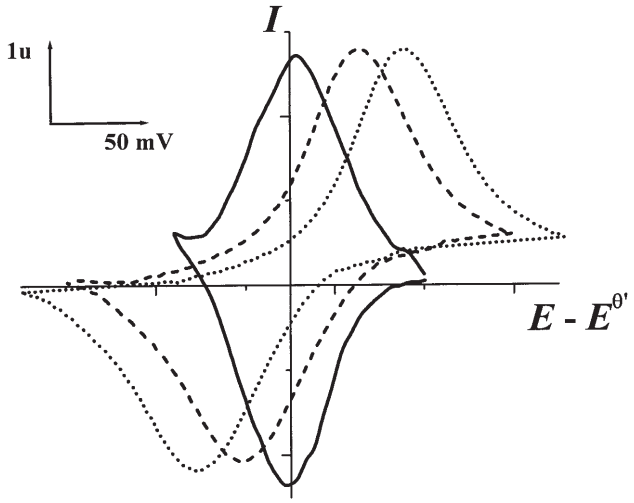

Fig. 5. Background-subtracted CV at (—) 0.005, (– – – –) 1.5, and (·····) 5 V s^{-1} of adsorbed P_{glivec} in pH 7.2 0.1 M phosphate buffer; 1 u of current represents 1.43 nA for 5 mV s^{-1}, 435 nA for 1.5 V s^{-1}, and 1.1 μA for 5 V s^{-1}.

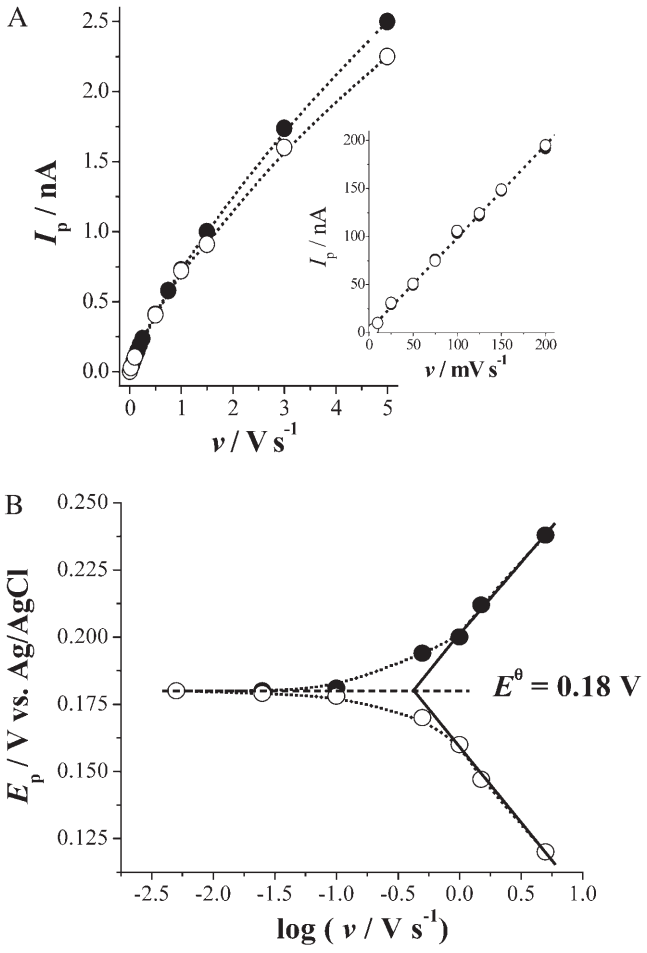

Fig. 6. A) Plot of (●) I_{pa} and of (○) I_{pc} of adsorbed P_{glivec} function of v. B) Plot of (●) E_{pa} and (○) E_{pc} of adsorbed P_{glivec} function of log v.

scan rates on the peak current (ohmic drop) due to uncompensated resistance of the solution between working and reference electrode [18].

The influence of the scan rate on the anodic and cathodic peak potentials of adsorbed P_{glivec} was also investigated for $5 \leq v \leq 5000$ mV s^{-1}, Figure 6A. For $5 \leq v \leq 30$ mV s^{-1} the peak potentials are not influenced by increasing scan rate.

For higher scan rates, $v \geq 300$ mV s^{-1}, the anodic and the cathodic peak potentials are displaced to more positive and to more negative values, respectively, following a linear relationship with log (v), Figure 6B. The slopes of these lines were calculated to be 59 mV/decade. The two oblique asymptotes corresponding to the variation of peak potentials with log (v) for high scan rate intersect at the same point, the horizontal asymptote corresponding to the variation of the peak potentials with log (v) for low scan rates.

According to theoretical predictions [22], the slope of the variation of peak potential with log (v) for scan rates, when the system is not reversible, is given by $-2.3\ RT(\alpha_c nF)^{-1}$ for the cathodic peak and by $-2.3\ RT[(1-\alpha_c)nF]^{-1}$ for the anodic peak where F is the Faraday constant, R the ideal gas constant, T the absolute temperature, α_c the cathodic transfer coefficient and n the number of electrons. In this particular case the sum of the anodic and cathodic transfer coefficients in unity. This allows the calculation of $\alpha_c n = 1$.

Also, the horizontal asymptote enables the determination of the surface standard potential $E^{\theta'} = +180$ mV which, in the case of a reversible reaction when $v \to 0$, is equal to E_{pa} and E_{pc}.

The intersection between the two linearly extrapolated lines occurs at log $v = -0.40$. This value corresponds to a scan rate of 0.40 V s^{-1}. Using the equation

$$k_0 = \alpha_c\ n\ F\ v_c\ (RT)^{-1} = \alpha_a\ n\ F\ v_a\ (RT)^{-1}$$

the standard rate constant of the electrochemical reaction, k_0 was calculated to be 15.5 s^{-1}.

3.4. Square-Wave Voltammetry

The advantage of using pulse voltammetric techniques for analytical and mechanistic studies is their ability to decouple the faradaic current from the capacitive current, especially in systems that involve adsorption of the reactants at the electrode surface [23, 24].

Another greater advantage of square-wave methods is the possibility to see during only one scan if the electron-transfer reaction is reversible or not. Since the current is sampled in both positive- and negative-going pulses, peaks corresponding to the oxidation and reduction of the electroactive species at the electrode surface can be obtained in the same experiment.

Square-wave voltammograms of adsorbed P_{glivec} were recorded in pH 4.7 0.1 M acetate buffer. For frequencies lower or equal to 50 Hz, one main oxidation peak was observed at $E_{pa} = +0.35$ V, and its current increased with

increasing frequency, Figure 7A. The identical value of the potential of the P_{glivec} peak on the forward and backward current components (not shown) is an indication that the process occurs only on the GCE surface.

Increasing the frequency, and holding the step potential and pulse amplitude constant, led to splitting of the total current showing the transformation of the system into an irreversible one by increasing the scan rate, Figure 7A. This behavior is reflected in the total current due to the progressive displacement of the peak potentials obtained on the forward and on the backward currents, Figure 7B, and is characteristic of reversible electrode processes when the electrochemical species is adsorbed at the electrode surface [23, 24].

3.5. Analytical Determination of Adsorbed Glivec

Graphical integration of the anodic current – potential curve obtained at $v = 5$ mV s^{-1} gives the total charge $Q = 3.5 \times 10^{-8}$ C transferred during P_{glivec} oxidation. Supposing that, during one scan, all the adsorbed molecules are oxidized, the surface concentration of adsorbed P_{glivec} can be calculated as $\Gamma_{Pglivec} = Q(nFA)^{-1} = 2.5 \times 10^{-12}$ mol cm^{-2}, where A is the geometrical electrode area in cm^2. The symmetry of the wave shape allows the calculation of the surface concentration using $I_{pa} = (4RT)^{-1}\ F^2n^2vA\Gamma_{Pglivec}$, if a Langmuir isotherm behavior is obeyed [18]. For $v = 5$ mV s^{-1} the peak current $I_{pa} = 3.3$ nA and therefore $\Gamma_{Pglivec} = 2.5 \times 10^{-12}$ mol cm^{-2}.

Quantitation of glivec in solution has been carried out using two different procedures. The first followed glivec oxidation peak in solutions with different glivec concentrations in pH 4.5 0.1 M acetate buffer. During this procedure pH 4.5 was used since previous results have shown that in this electrolyte higher glivec peaks can be obtained. The second procedure followed the oxidation peak of adsorbed P_{glivec} in pH 7.2 0.1 M phosphate buffer since it was shown in Section 3.2 that in this electrolyte higher P_{glivec} oxidation peaks were obtained. Adsorption of P_{glivec} at the GCE surface was carried out from the glivec solution as described in Section 2.4, Procedure 3.

A linear dependence, Figure 8, of glivec oxidation peak current with concentration was obtained between 0.04 μM up to 1 μM, given by the equation I_{pa} (nA) $= 0.94 + 29.6\ C_{Glivec}$ ($R = 0.9998$, $N = 9$, $S.D. = 0.33$). For the P_{glivec} peak, the concentration range of current linearity was 0.005 μM $\leq C_{Glivec} \leq 0.100$ μM and the equation was: I_{pa} (nA) $= 2.61 + 205\ C_{Glivec}$ ($R = 0.9999$, $N = 7$, $S.D. = 0.02$).

The sensitivity for the detection of glivec using the described method can be demonstrated by determining the limit of detection (LOD). The LOD was determined as the drug concentration that caused a peak with a height three times the baseline noise level. Using the line param-

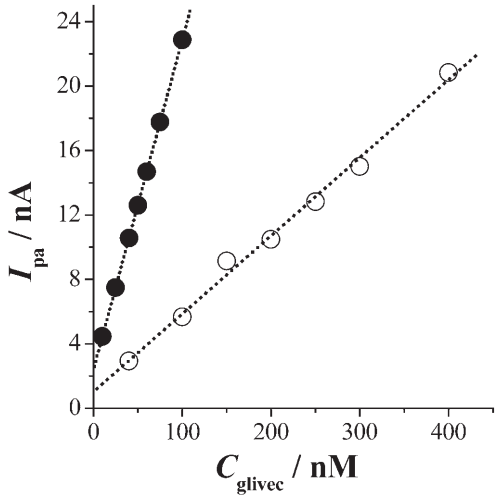

Fig. 8. Plot of I_{pa} of (○) glivec oxidation peak in pH 4.5 0.1 M acetate buffer and of (●) P_{glivec} oxidation peak in pH 7.2 0.1 M phosphate buffer. Adsorption of P_{glivec} at the GCE surface was carried out as described in Procedure 3, Section 2.4.

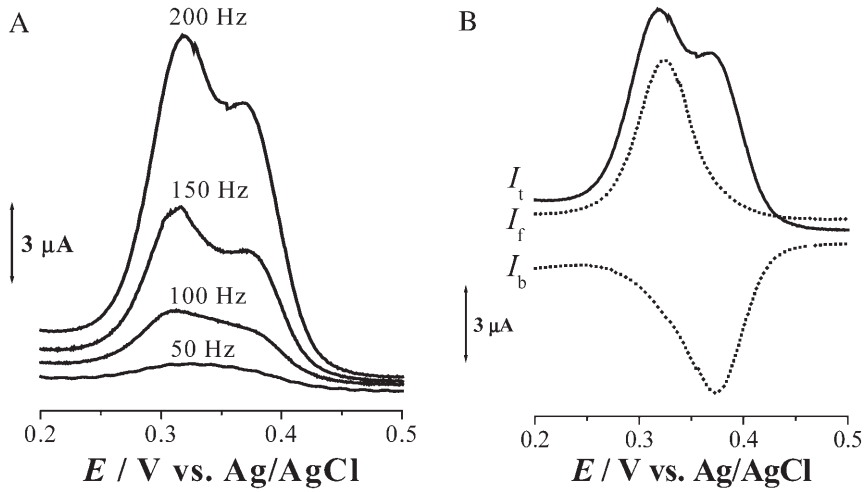

Fig. 7. SWV at A) increasing frequency and B) $v_{effective} = 200$ mV s^{-1} ($f = 200$ Hz, $\Delta E_s = 1$ mV) of adsorbed P_{glivec} in pH 4.3 0.1 M acetate buffer.

eters of $I_{pa} = I_{pa}$ (C_{Glivec}), the obtained LOD following peak 1_a was $LOD_{glivec} = 3.3 \times 10^{-8}$ M, whereas following peak 3_a the detection limit was $LOD_{Pglivec} = 2.9 \times 10^{-10}$ M.

The quantitation limit (LOQ) is the lowest concentration of a substance that can be quantitated with acceptable precision and accuracy. A typical signal/noise ratio of 10 is generally considered to be acceptable; therefore: $LOQ_{glivec} = 1.1 \times 10^{-7}$ M and for peak 3_a $LOQ_{Pglivec} = 0.97 \times 10^{-9}$ M.

4. Conclusions

The antileukemia drug glivec undergoes oxidation at glassy carbon electrodes and involves the formation of an oxidation product, P_{glivec}. The adsorption of P_{glivec} at the GCE surface yields a compact monolayer that inhibits further oxidation of glivec.

Due to the strong adsorption of P_{glivec} at the electrode surface, a detailed electrochemical study of this compound adsorbed at the GCE surface was carried out over a large pH range. The reversible redox reaction of the adsorbed P_{glivec} is pH dependent and occurs with the transfer of 2 electrons and 2 protons. Using cyclic voltammetry, the surface standard potential and the rate constant of the heterogeneous electrochemical reaction were calculated to be $E^{\circ\prime} = +180$ mV and $k = 15.5\ s^{-1}$, respectively. The total surface concentration of adsorbed P_{glivec} was also calculated to be 2.5×10^{-12} mol cm^{-2}. The analytical determination of glivec was carried out by differential pulse voltammetry by measuring the anodic peak current corresponding to either the oxidation of glivec or the oxidation of P_{glivec} adsorbed on the GCE surface. The limits of detection of glivec and adsorbed P_{glivec} based on three times the noise level were 3.3×10^{-8} M and 2.9×10^{-10} M, respectively.

5. Acknowledgements

Financial support from Fundação para a Ciência e Tecnologia (FCT), Post-Doctoral Grant SFRH/BPD/18824/2004 (V. C. Diculescu.), POCTI (cofinanced by the European Community Fund FEDER), and ICEMS (Research Unit 103).

6. References

[1] The Glivec International Site, *http://www.glivec.com/about*.
[2] D. Moffat, P. Davis, M. Hutchings, J. Davis, D. Berg, M. Batchelor, J. Johnson, J. O'Connell, R. Martin, T. Crabbe, J. Delgado, M. Perry, *Bioorg. Med. Chem. Lett.* **1999**, *9*, 3351.
[3] E. Buchdunger, A. Matter, B.J Druker, *Biochim. Biophys. Acta*. **2001**, *1551*, M11.
[4] D. L. Stirewalt, S. Meshinchi, J. P. Radich, *Blood Rev.* **2003**, *17*, 15.
[5] P. Zhang, W. Y. Gao, S. Turner, B. S. Ducatman, *Mol. Cancer* **2003**, *2*, 1.
[6] J. Li, J. Kleeff, J. Guo, L. Fischer, N. Giese, M. W. Büchler, H. Friess, *Mol. Cancer*, **2003**, *2*, 1.
[7] G. W. Krystal, *Drug Resist. Updat.* **2001**, *4*, 16.
[8] E. Weisenberg, J. D. Griffin, *Drug Resist. Updat*. **2001**, *4*, 22.
[9] G. Hoser, I. Majsterek, D. L. Romana, A. Slupianek, J. Blasiak, T. Skorski, *Leukem. Res.*, **2003**, *27*, 267.
[10] R. Bakhtiar, J. Lohne, L. Ramos, L. Khemani, M. Hayes, F. Tse, *J. Chromatogr. B.* **2002**, *768*, 325.
[11] R. A. Parise, R. K. Ramanathan, M. J. Hayes, M. J. Egorin, *J. Chromatogr. B.* **2003**, *791*, 39.
[12] R. Bakhtiar, L. Khemani, M. Hayes, T. Bedman, F. Tse, *J. Pharm. Biomed. Anal*. **2002**, *28*, 1183.
[13] G. Guetens, G. De Boeck, M. Highley, H. Dumez, A. T. Van Oosterom, E. A. de Bruijn, *J. Chromatogr. A*. **2003**, *1020*, 27.
[14] D. Ivanovic, M. Medenica, B. Jancic, A. Malenovic, *J. Chromatogr. B.* **2004**, *800*, 253.
[15] J. R. Flores, J. J. Berzas, G. Castaneda, N. Rodriguez, *J.Chromatogr. B.* **2003**, *794*, 381.
[16] A. M. Oliveira Brett, J. A. P. Piedade, A. M. Chiorcea, *J. Electroanal. Chem*. **2002**, *538–539*, 267.
[17] J. Rodriguez, J. J. Berzas, G. Castaneda, N. Rodriguez, *Talanta* **2005**, *66*, 202.
[18] C. M. A. Brett, A. M. Oliveira Brett, *Electrochemistry: Principles, Mmethods and Applications*, Oxford Science University Publications, Oxford **1993.**
[19] E. Laviron, *J. Electroanal. Chem*. **1974**, *52*, 355.
[20] A. T. Hubbard, F. C. Anson, in *Electroanalytical Chemistry*, Vol. 4 (Ed: A. J. Bard), Marcel Dekker, New York **1970**, p. 129.
[21] A. P. Brown, F. C. Anson, *Anal. Chem*. **1977**, *49*, 1589.
[22] E. Laviron, *J. Electroanal. Chem*. **1979**, *101*, 19.
[23] J. J. O'Dea, J. Osteryoung, R. A. Osteryoung, *Anal. Chem*. **1981**, *53*, 695.
[24] J. Osteryoung, R. Osteryoung, *Anal. Chem*. **1985**, *57*, 101A.

